How Foam Develops Apparent Viscosity in EOR

George J. Hirasaki
Rice University

September 26, 2025

3rd International Whole Value Chain CCUS Conference Week in Golden, CO

Abstract

Foam is a process used for mobility control in enhanced oil recovery and aquifer remediation. While simple in concept and execution, it often is not optimally applied because of limitations in the understanding of how it functions. This presentation highlights some of the findings discovered during 45 years of my research with foam EOR and aquifer remediation.

Outline

- Current state of the art
- Choice of surfactant
- Smooth capillaries
- Effect of constrictions
- Foam texture
- Mechanisms for foam generation
- Mechanisms for foam destruction
- Population balance simulation
- Minimum pressure gradient for foam generation
- Empirical foam model for reservoir simulation
- Experiments and simulations for field application
- Conclusions

Current state of the art: Measurements and modeling

Effect of permeability on apparent viscosity

$$\mu_f^{app} \equiv \frac{k}{\left(u_w + u_g\right)} \frac{\Delta p}{L}$$

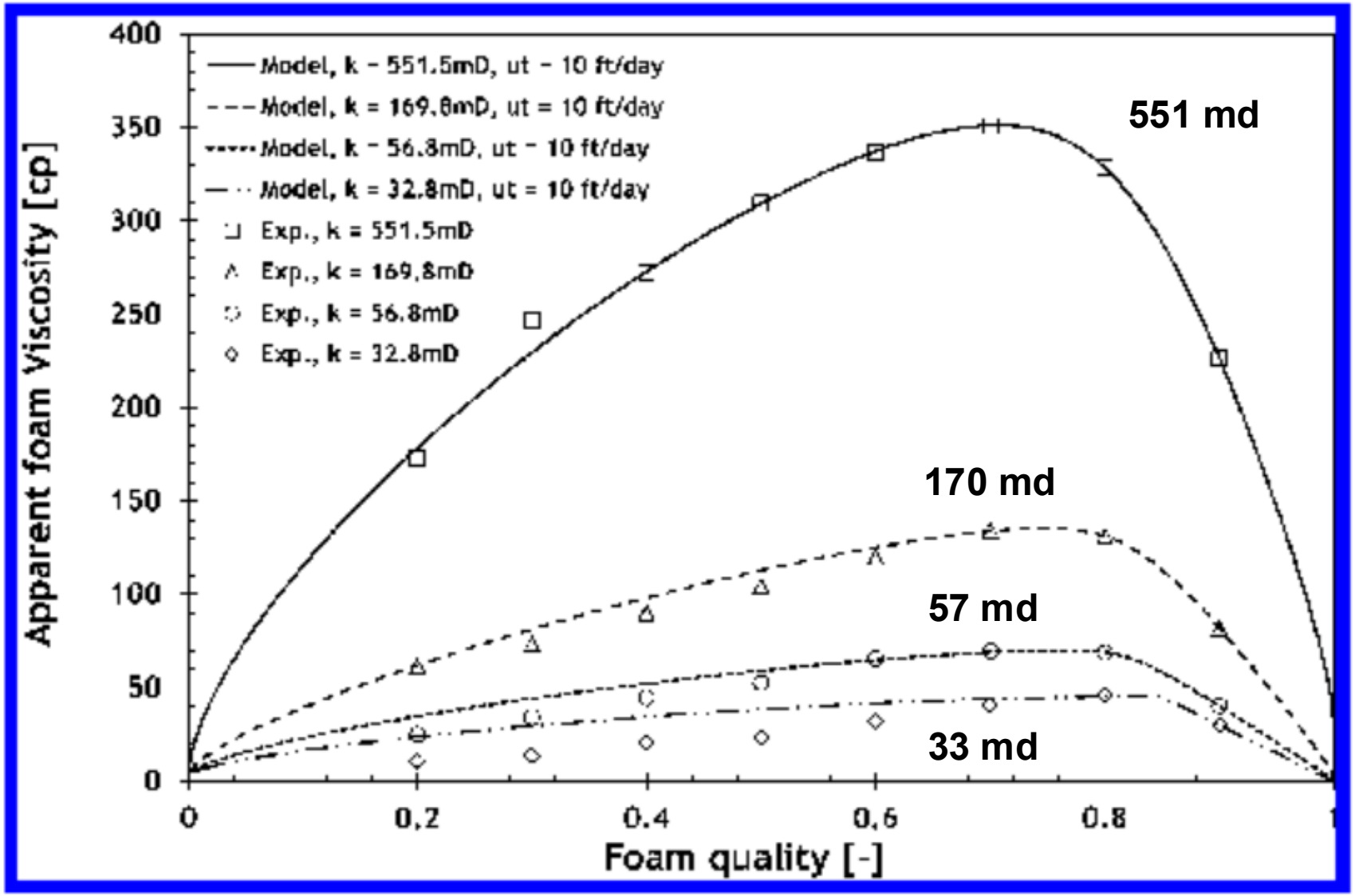

Figure 3. Apparent viscosity of CO_2 foam made with 2000 ppm of Chaser CD-1050 as a function of permeability.

Farajzadeh, et al., 2015, *Energy & Fuels, 29*, 3011-3018.

Choice of surfactant

- Reservoir: sandstone or carbonate, salinity, temperature
- Type of surfactant
  - Anionic: sulfonate, sulfate, ethoxy- sulfate, ethoxy- carboxylate
  - Nonionic: ethoxylated alcohol, glucoside
  - Cationic: amine, diamine
  - Zwitterionic: betaine, amido-betaine, sulfo-betaine
- Carbon number of surfactant, C12 → C18
- Low adsorption on formation minerals
- Chemical, physical, and biological stability
- Negligible partition into oil phase

Elhag, et al., 2014.
Chen, et al., 2015.
Svorstoel, I., et al., 1996.

Rossen, W.R., Farajzadeh, R.,
and Hirasaki, G.J., (2022),

How does foam gain flow resistance?

Smooth capillaries

Contributors to flow resistance

Hirasaki and Lawson, 1985, *SPEJ*

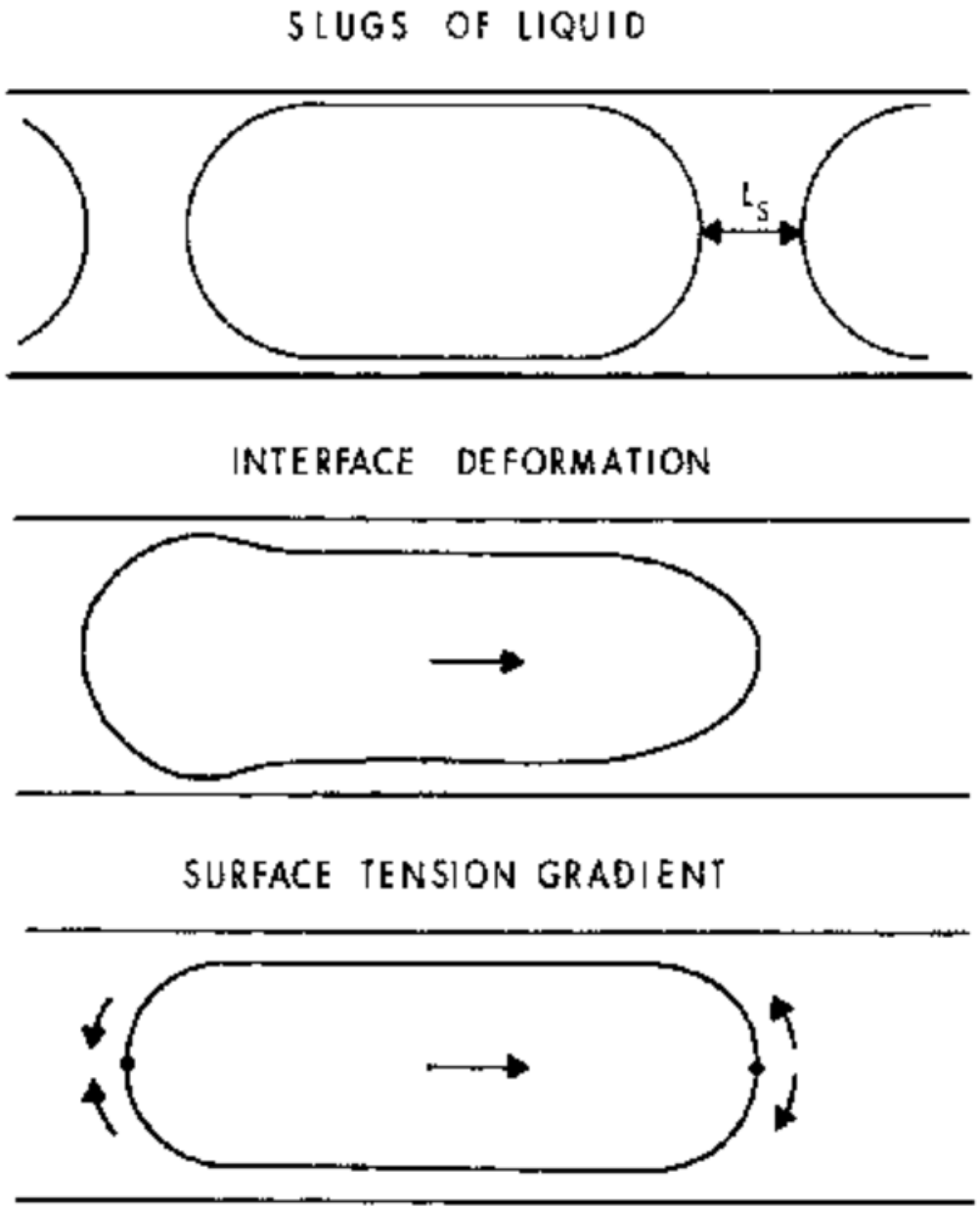

Fig. 1—Mechanisms affecting apparent viscosity in smooth capillaries.

Smooth capillaries

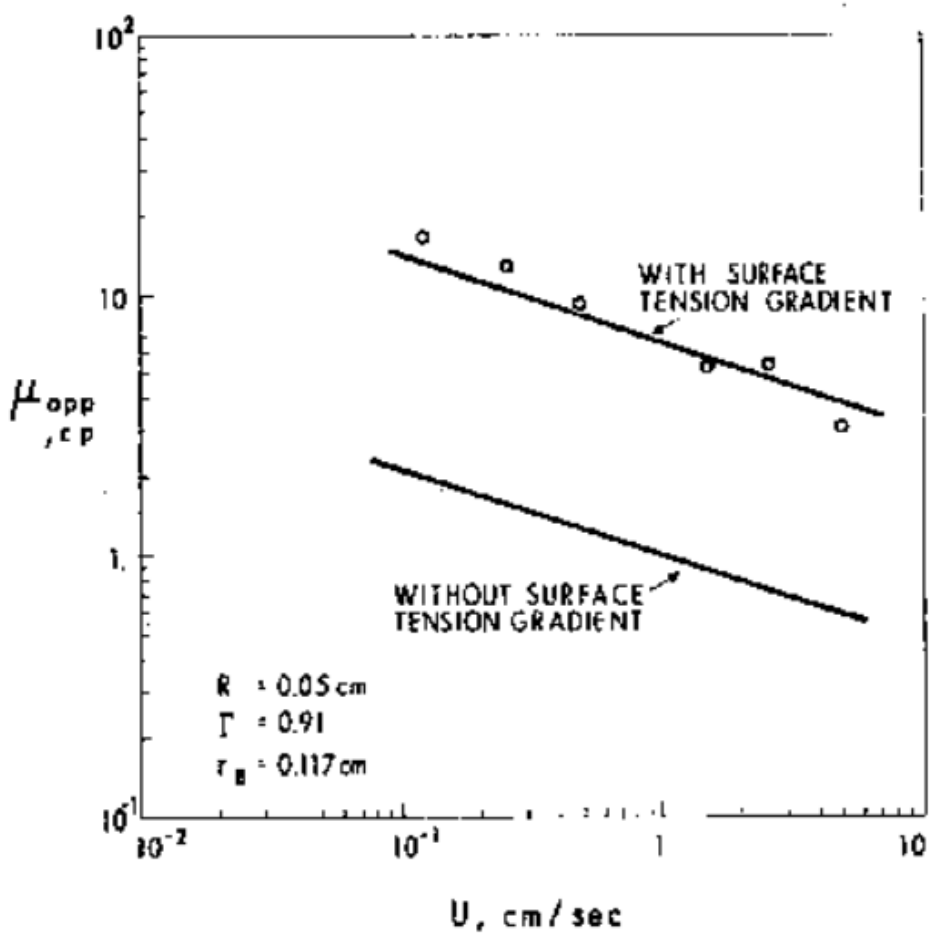

Fig. 10—Effect of surface tension gradient on apparent viscosity.

Hirasaki and Lawson, 1985, *SPEJ*

μ_f^{app}, cP

Apparent viscosity relative to Poiseuille law

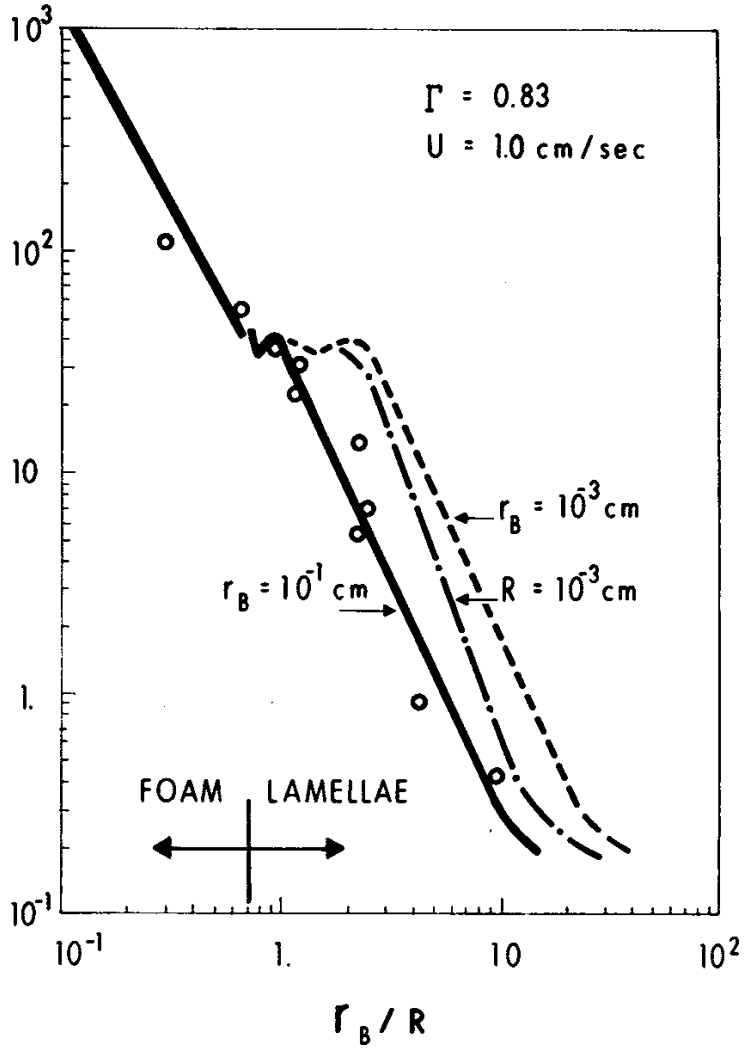

Combined effects of bubble size and capillary radius

Effect of constrictions

Bubbles in smooth capillaries are power-law fluid.

Pore constrictions have increasing effect at lower velocities and result in gas trapping

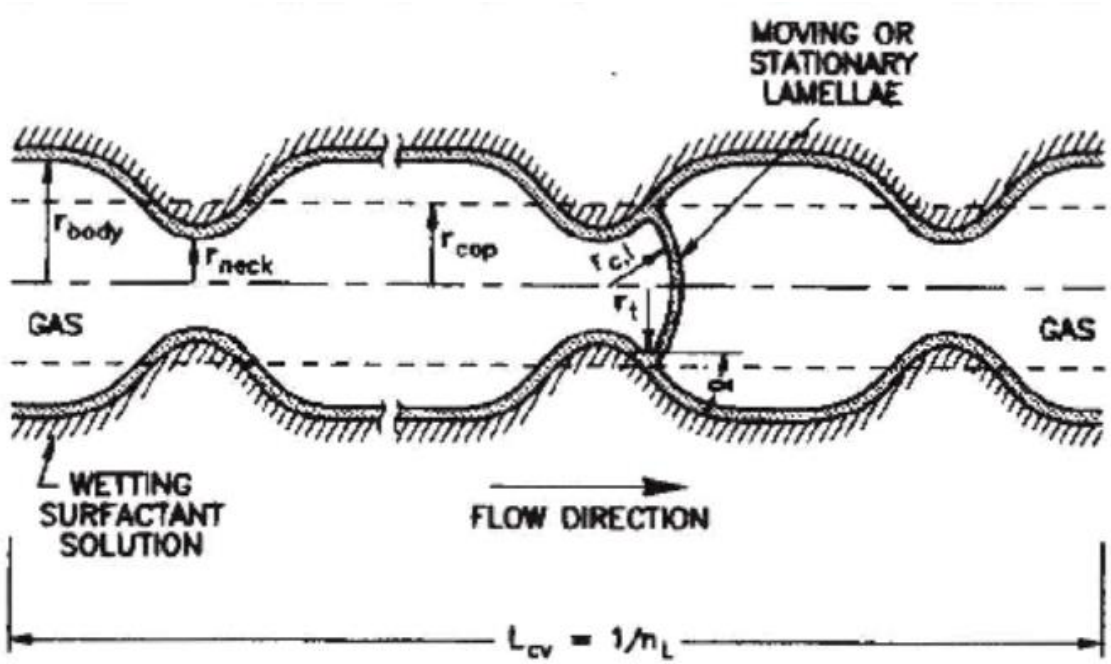

A.H. Falls, et al., 1989, *SPERE*

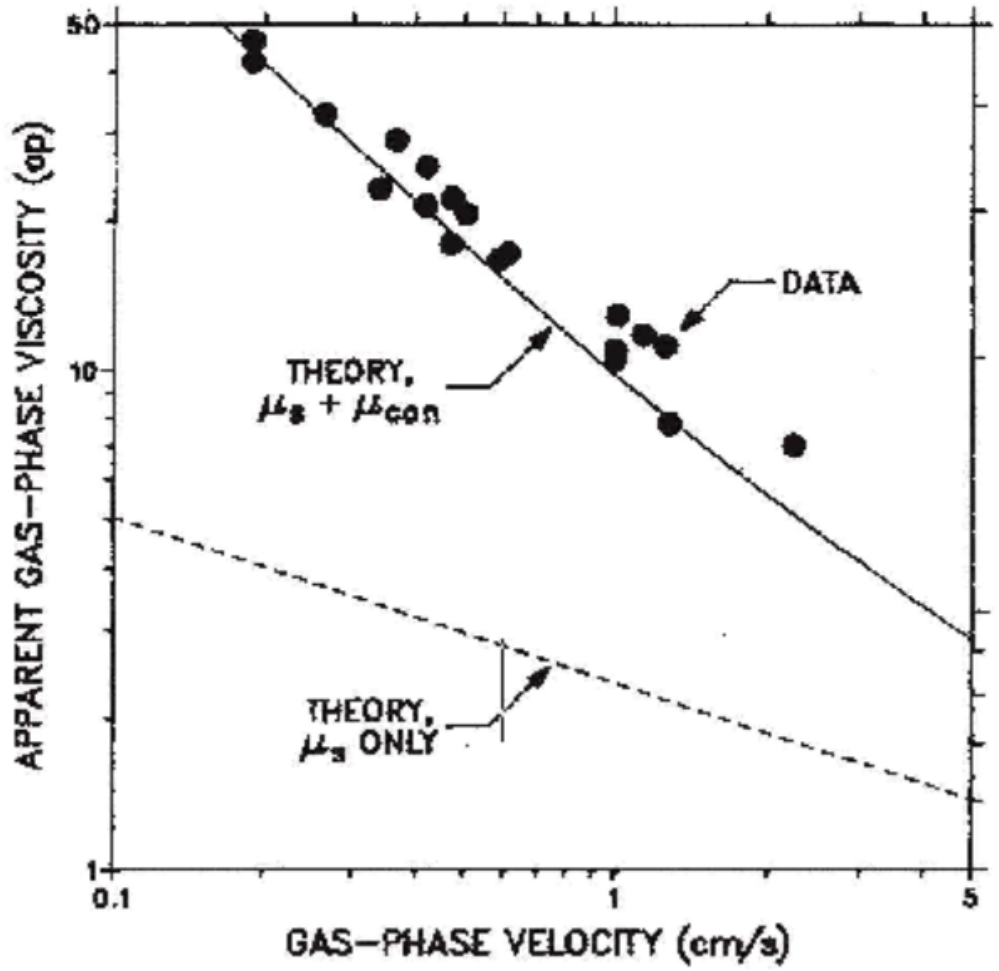

Foam texture

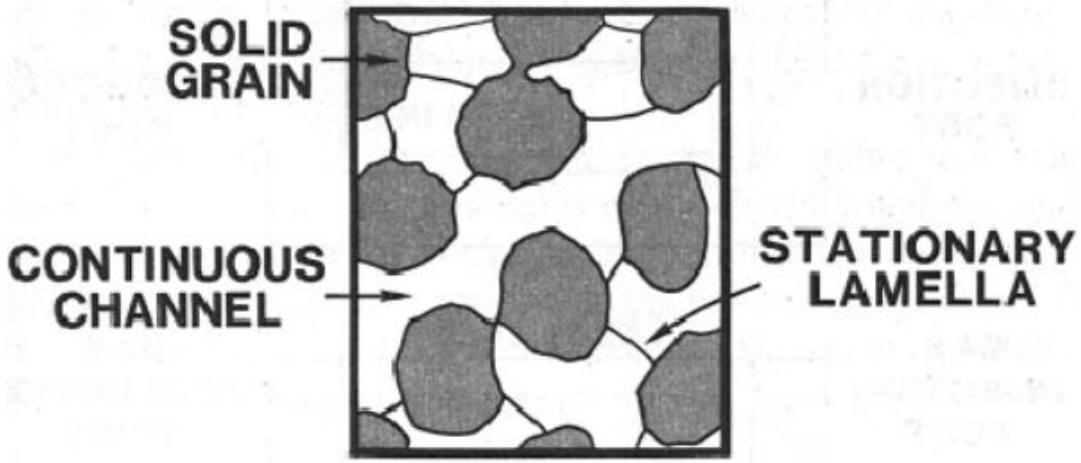

Continuous-gas foam

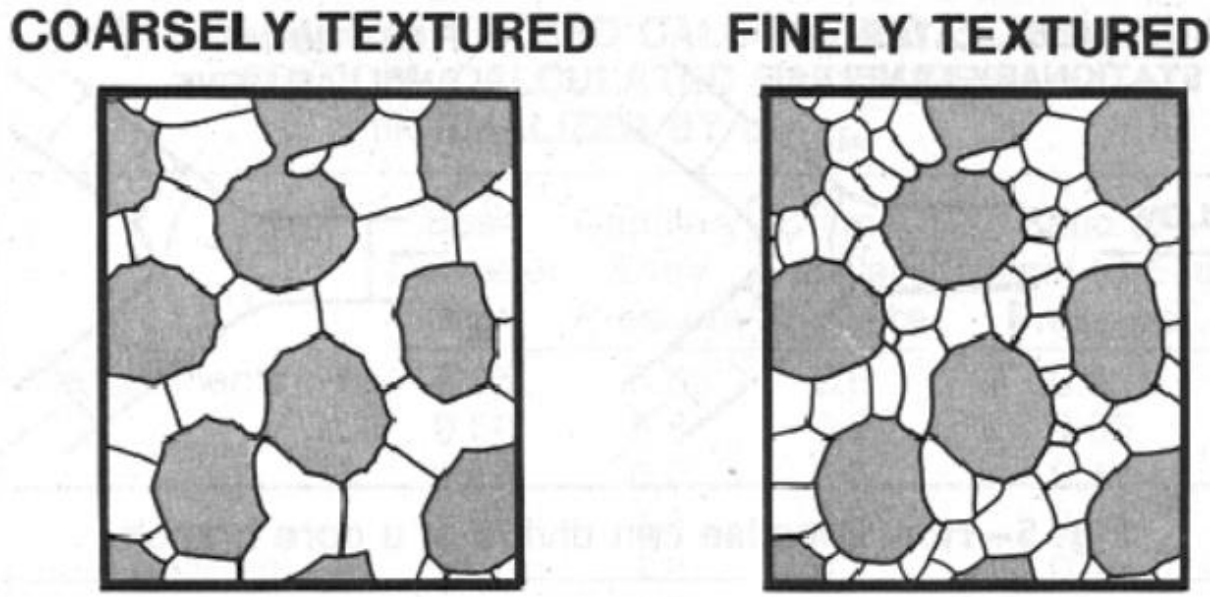

Discontinuous-gas foam

A.H. Falls, et al., 1988, *SPERE*, Aug.

Foam in sandpack with increasing foam quality

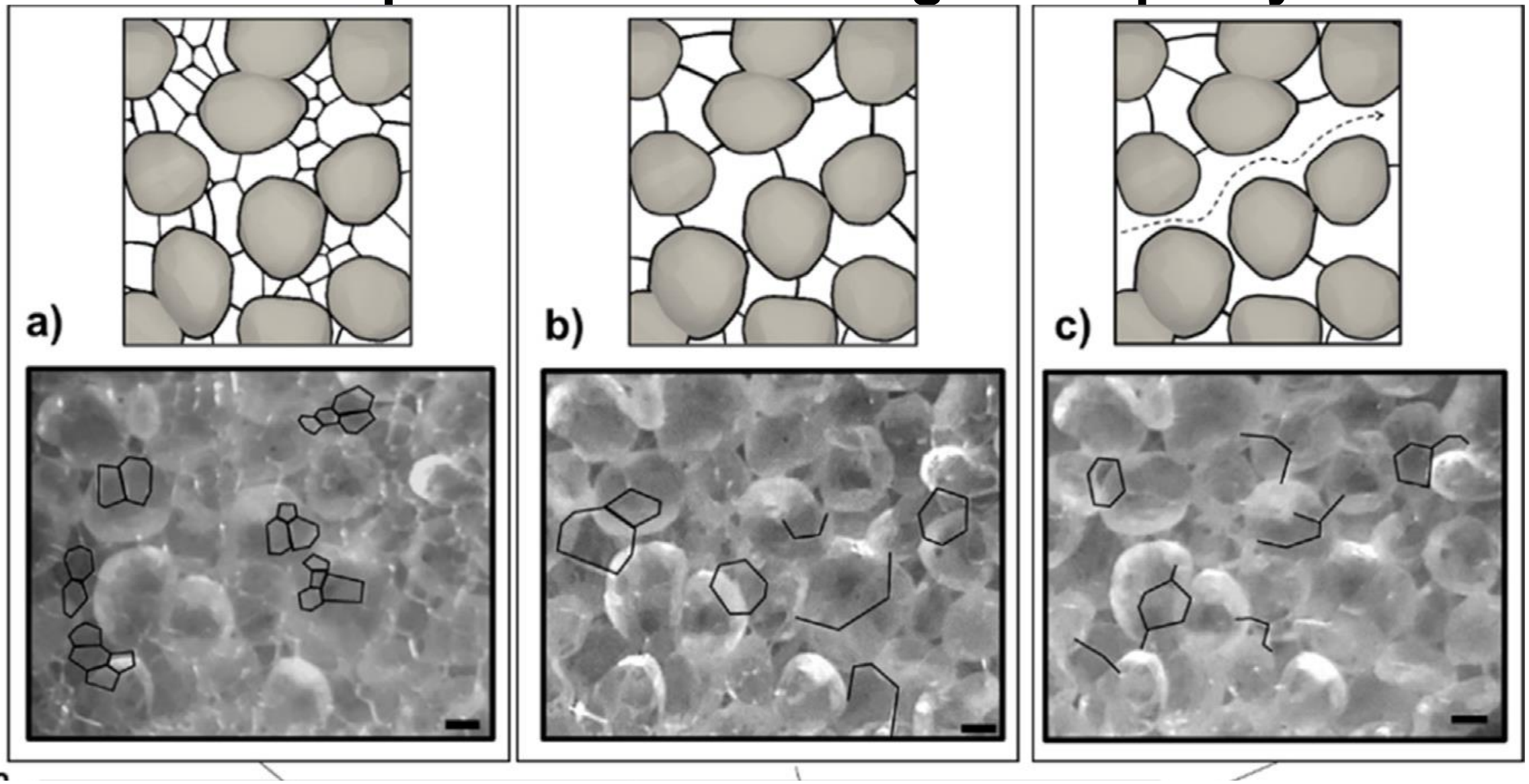

Vavra, et al., 2022

Capillary pressure as a function of foam quality (gas fractional flow)

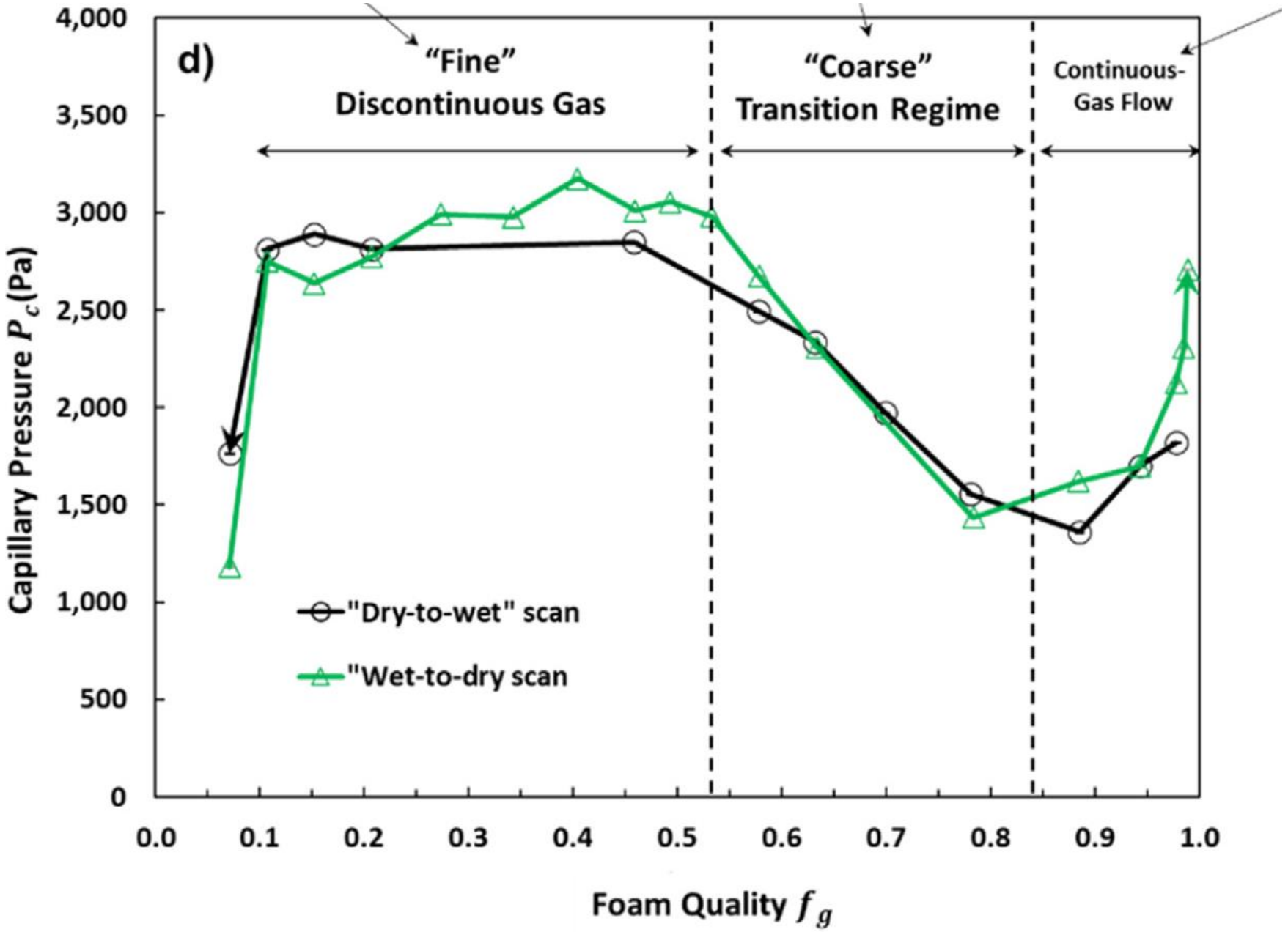

Vavra, et al., 2022

Mechanisms for foam generation

- Capillary snap-off
  - Pore body/throat contrast and water saturation
  - Capillary pressure for snap-off is < one-half of capillary entry pressure
  - Spontaneous migration of water from larger to smaller pores
  - Typical non-wetting phase residual saturation for:
    - Uniform bead pack: (B/T ~1) ~ 5%
    - Sandpack (B/T ~1) ~10%
    - Bentheimer (B/T ~1.2) ~20%
    - Berea sandstone (B/T ~5) ~40%
    - Vuggy carbonates ~50%
  - Inference: Capillary snap-off occurs more readily with large B/T ratio

  - Permeability contrast and water saturation

Mechanisms for foam generation

- **Bubble or lamella division**
  - **Branch points in flowing train of bubbles offer opportunity for bubble or lamellae division**
  - **Responsible for transition from continuous-gas foam to discontinuous-gas foam**

Low pressure gradient **Higher pressure gradient**

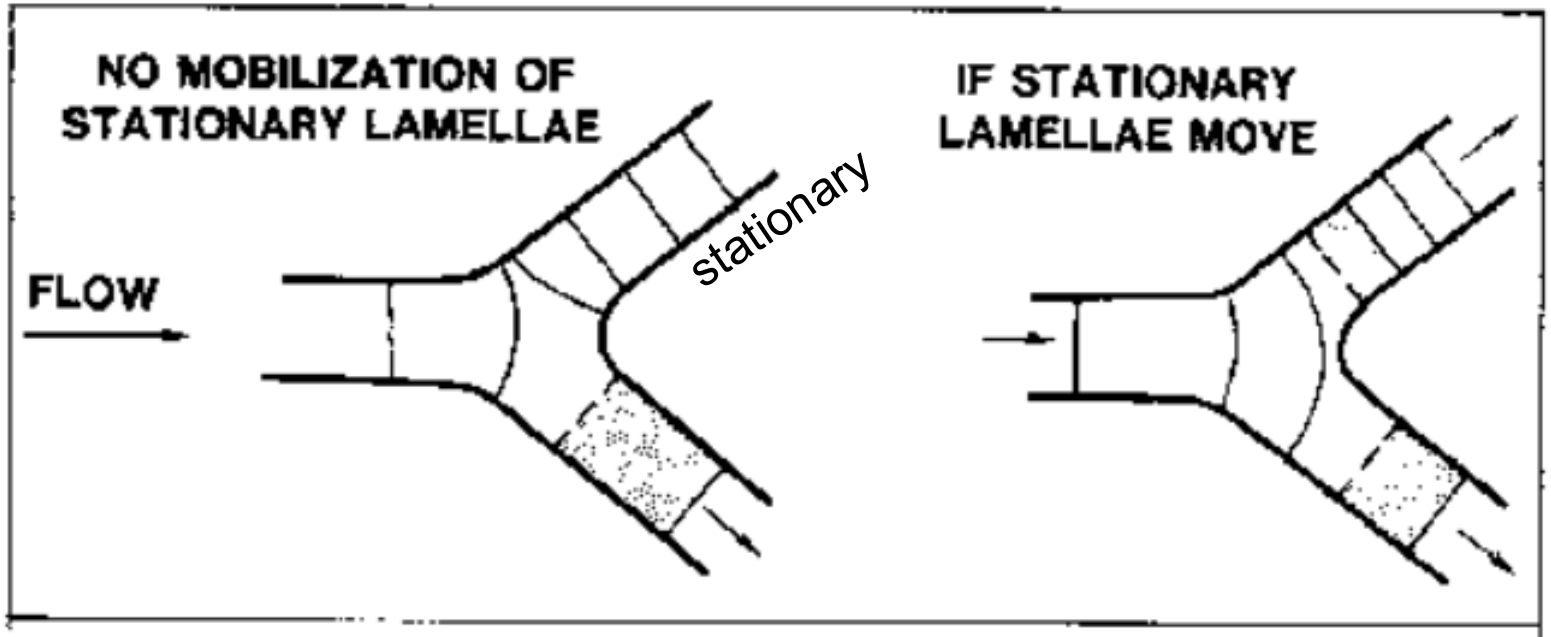

Fig. 5—How lamellae can divide at a pore branch.

A.H. Falls, et al., 1988, *SPERE*, Aug.

Mechanisms for foam generation

- **Capillary snap-off**

Pore constriction

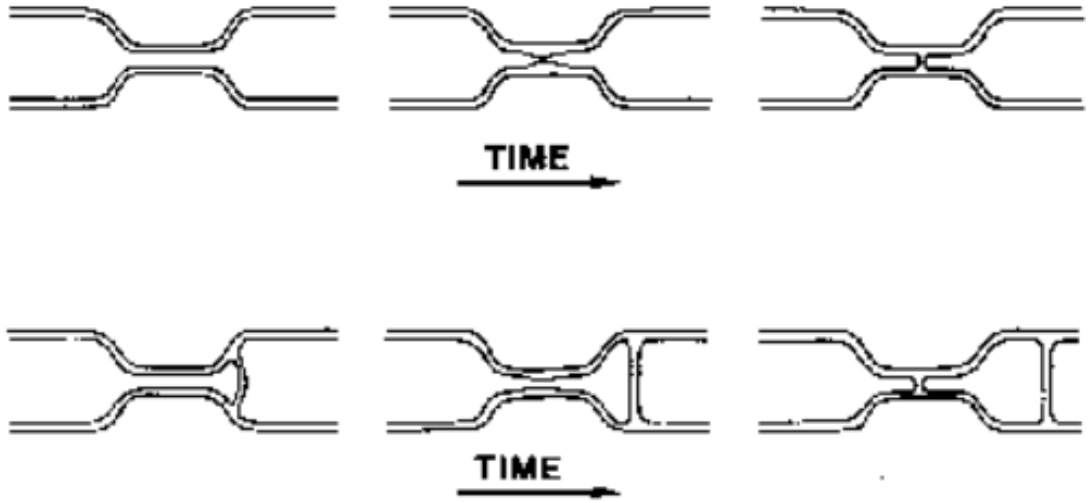

Fig. 4—How capillary snap-off can generate foam lamellae in a constricted capillary tube.

Permeability contrast

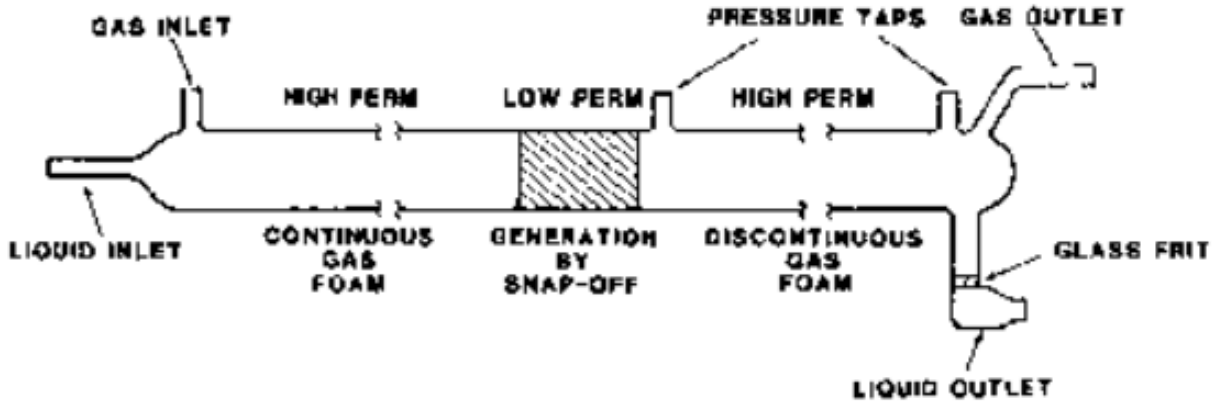

Fig. 7—Bead pack consisting of a low-permeability zone between two sections of higher permeability.

A.H. Falls, et al., 1988, *SPERE*, Aug.

Mechanisms for foam destruction

- Capillary pressure, P_c exceeds maximum stable disjoining pressure. This limits bubble refinement.
- Mass transfer from small bubbles to large bubbles
- Spreading of oil at gas/water interface

Population balance of bubble sizes

- Flowing and stationary gas bubbles
- Size distributions or mean value of bubble size
- Bubble density, i.e., number of bubbles per unit volume of gas
- Accumulation = -Divergence of flux + generation – destruction
- Mass balance for two phase flow
- Momentum balance; Darcy law

Population balance

A.H. Falls, et al., 1988, *SPERE*, Aug.

Generation only by snap-off

Grain sizes, 4:1

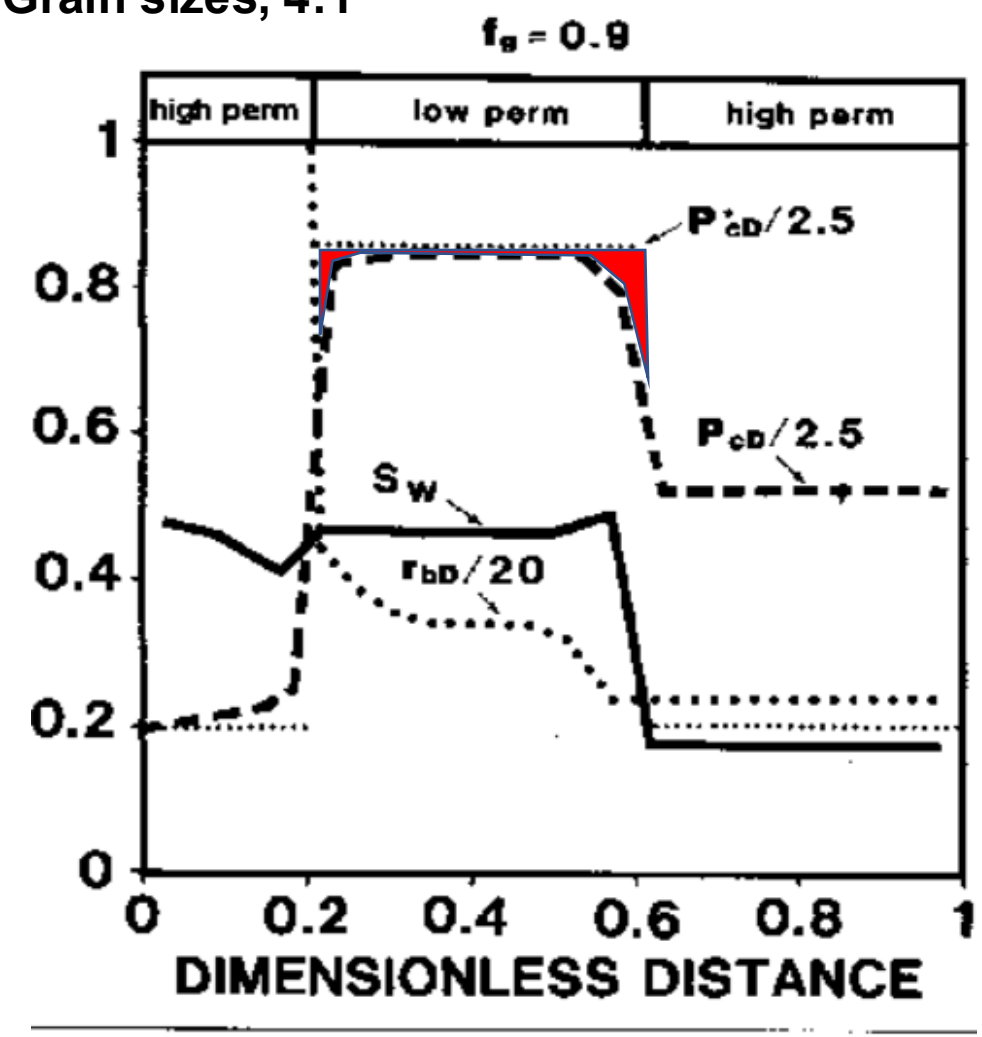

Fig. 9—Profiles of liquid saturation, capillary pressure, and bubble size simulated for $f_g = 0.9$.

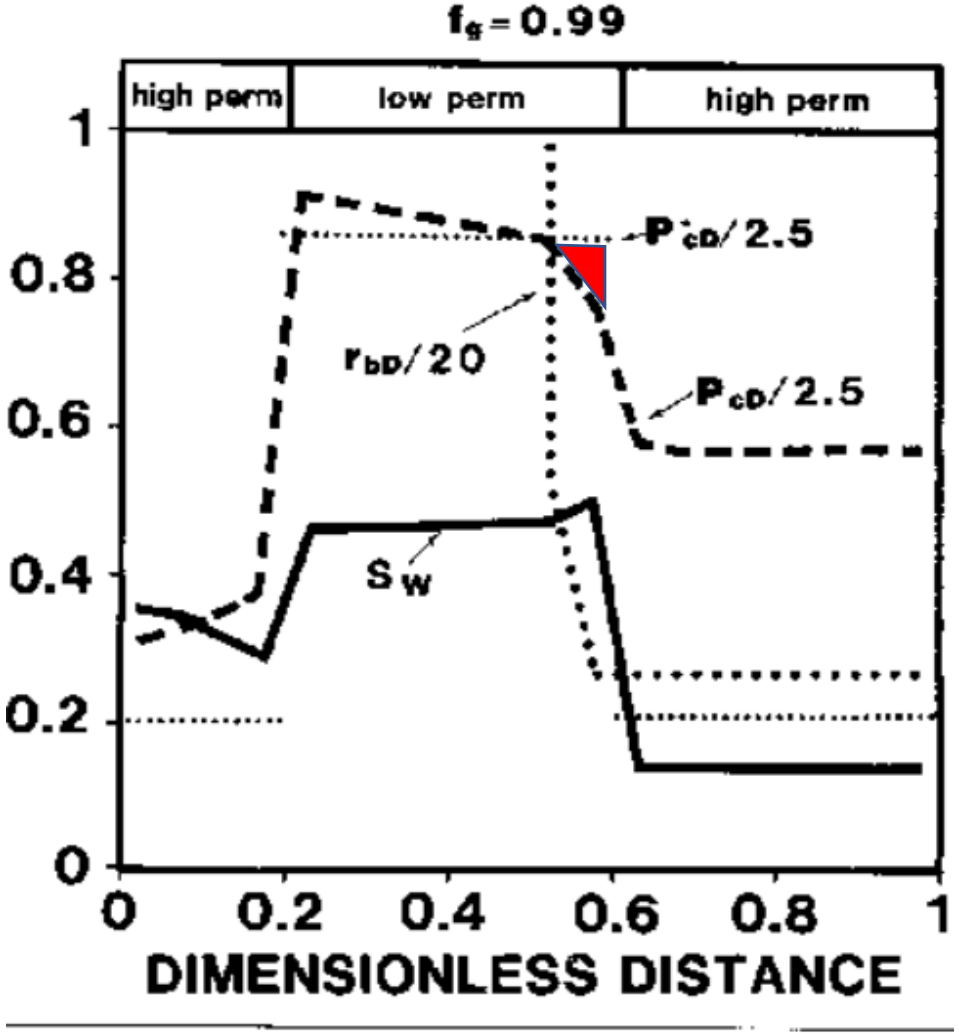

Fig. 8—Simulated profiles of liquid saturation, normalized capillary pressure, and normalized bubble size for $f_g = 0.99$.

Illustration of foam in homogeneous and heterogeneous sandpacks
(weakly foaming surfactant for aquifer remediation)

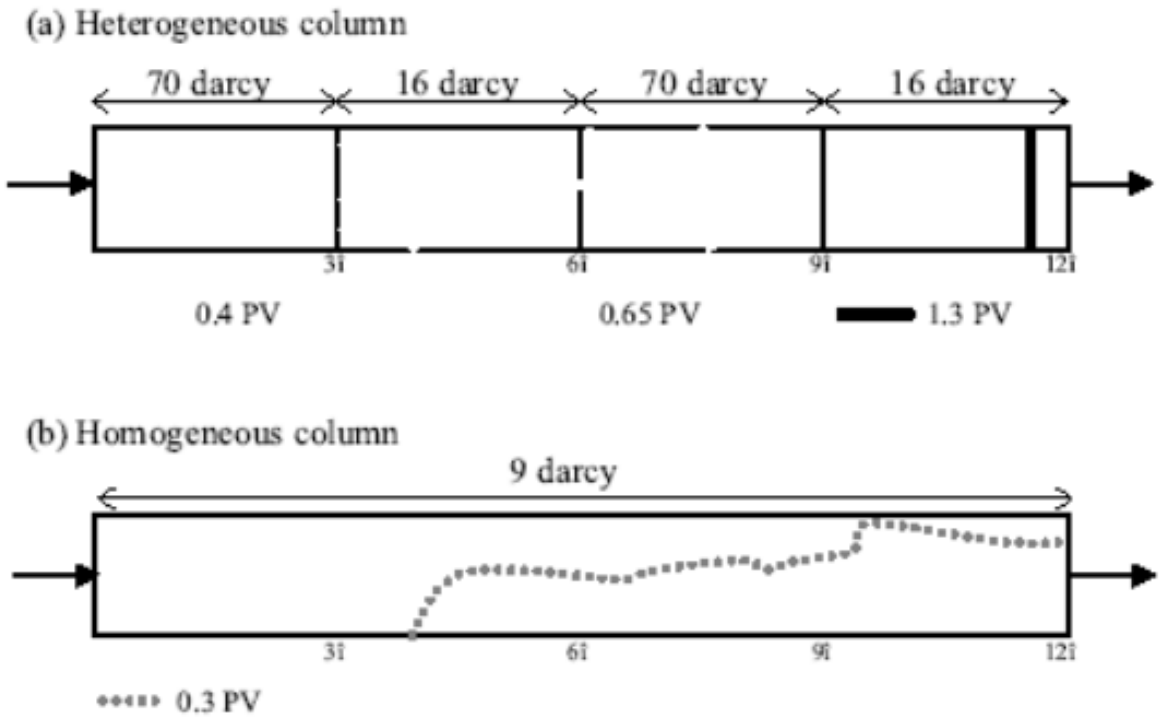

Fig. 11—Location and shape of the gas displacement front during transient foam experiments in (a) heterogeneous column with alternating high and low permeabilities, and (b) homogeneous column with low permeability. f_g=67% and u_g=0.6 ft/day.

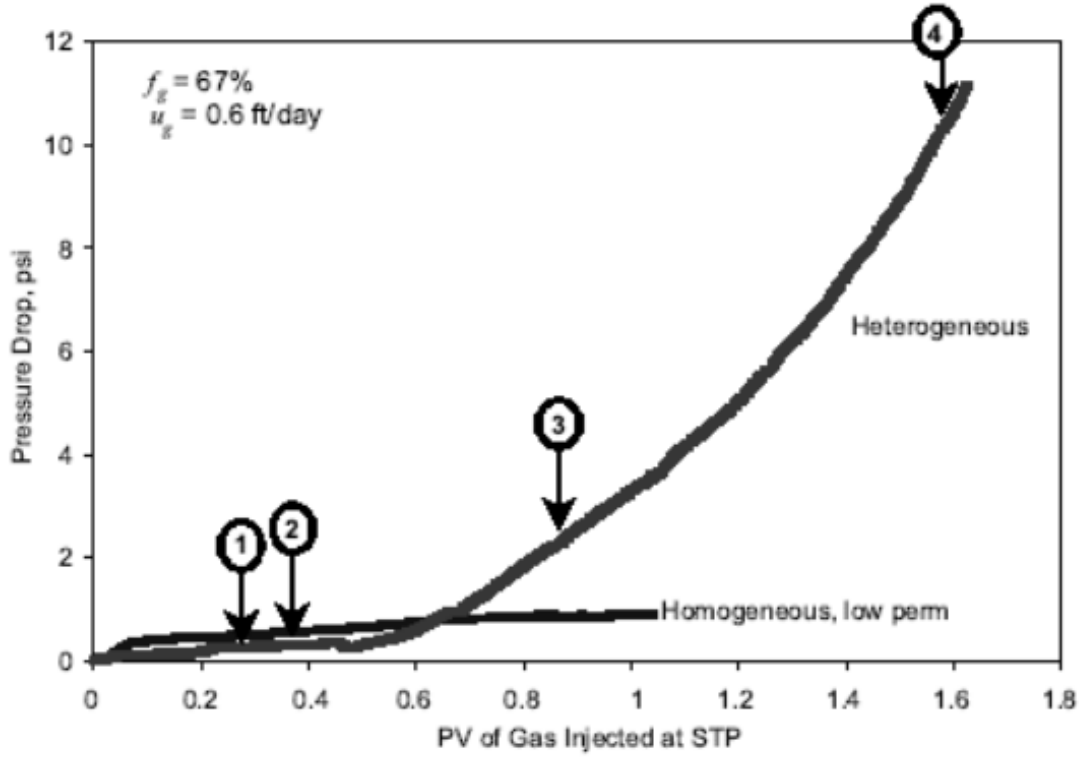

Fig. 12—Pressure drop during transient foam experiments with f_g=67% and u_g=0.6 ft/day in the heterogeneous (thick solid) and homogeneous (thin solid) columns. Arrows indicate the positions of gas front in the heterogeneous column at given times: (1) gas enters the fine sand section, (2) gas enters the coarse sand section and forms a strong foam front, (3) the strong foam front enters the last fine sand section, and (4) gas breaks through.

Tanzil, et al., 2002, June, SPEJ

Minimum pressure gradient for foam generation

Transition from continuous-gas foam to discontinuous-gas foam has a jump in pressure gradient when the minimum pressure gradient is exceeded.

f_g = 88%, C_s = 0.3%
AOS 14-16
Bentheimer sandstone

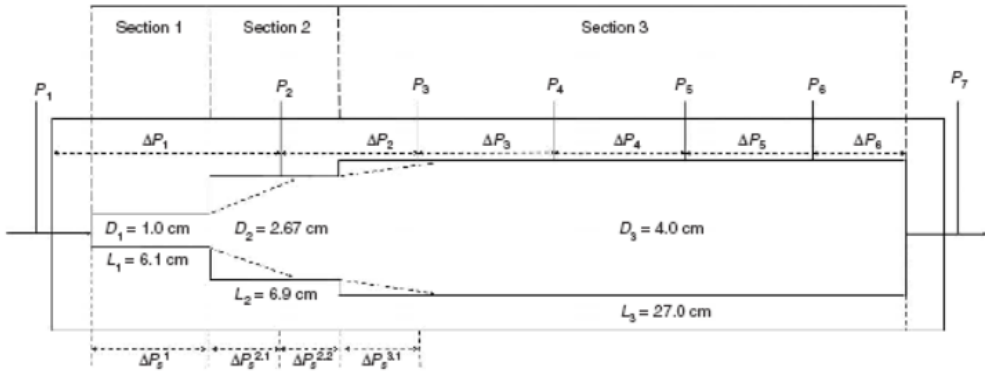

Fig. 3—Schematic illustration of core geometry.

Yu, Vincent-Bonnieu, Rossen, 2020, Dec., SPEJ

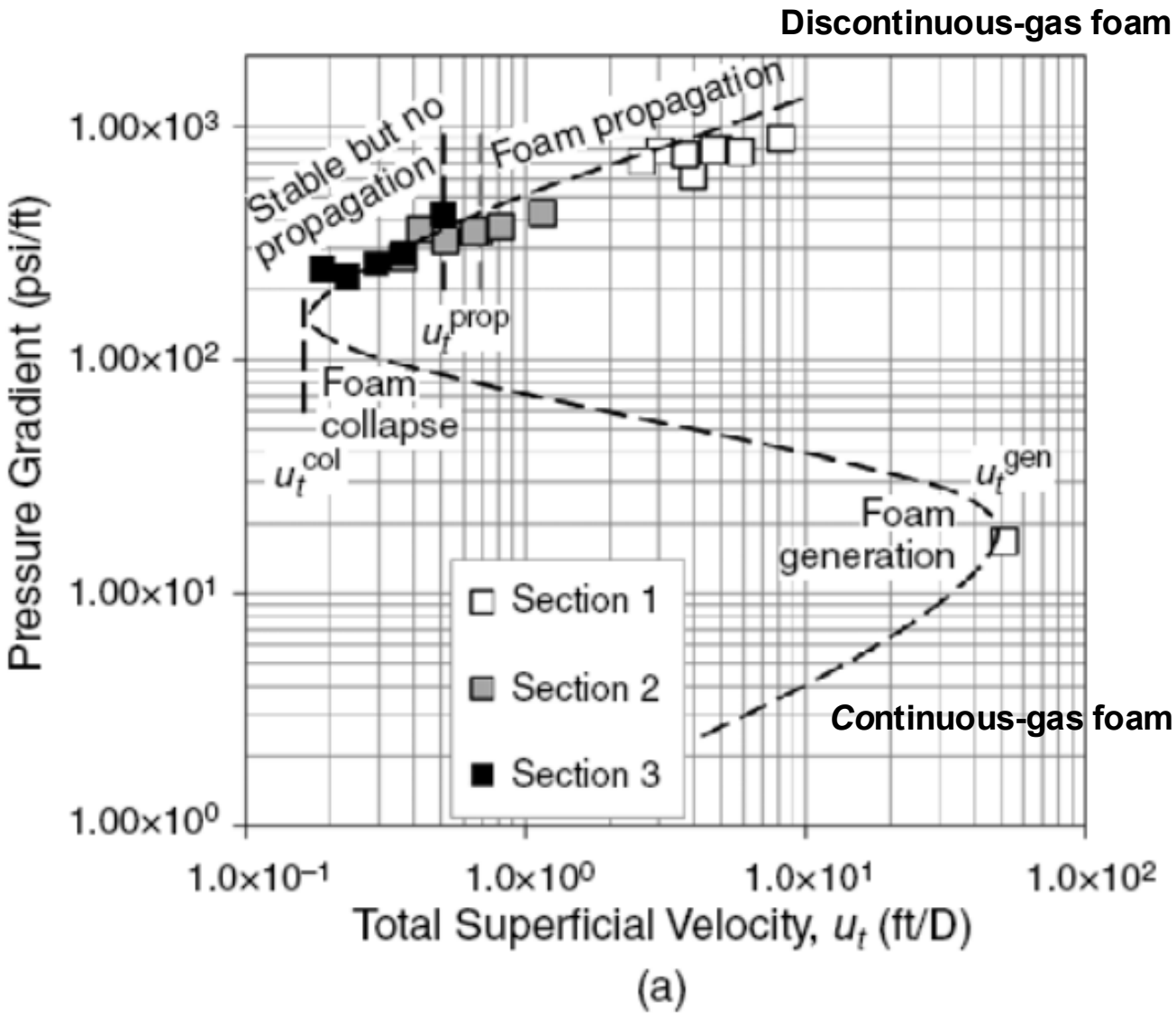

Foam apparent viscosity and capillary pressure as a function of foam quality, f_g and flow rate

1% AOS 14-16
in 143 darcy sandpack,
Constant u_g multiples

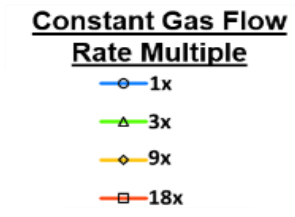

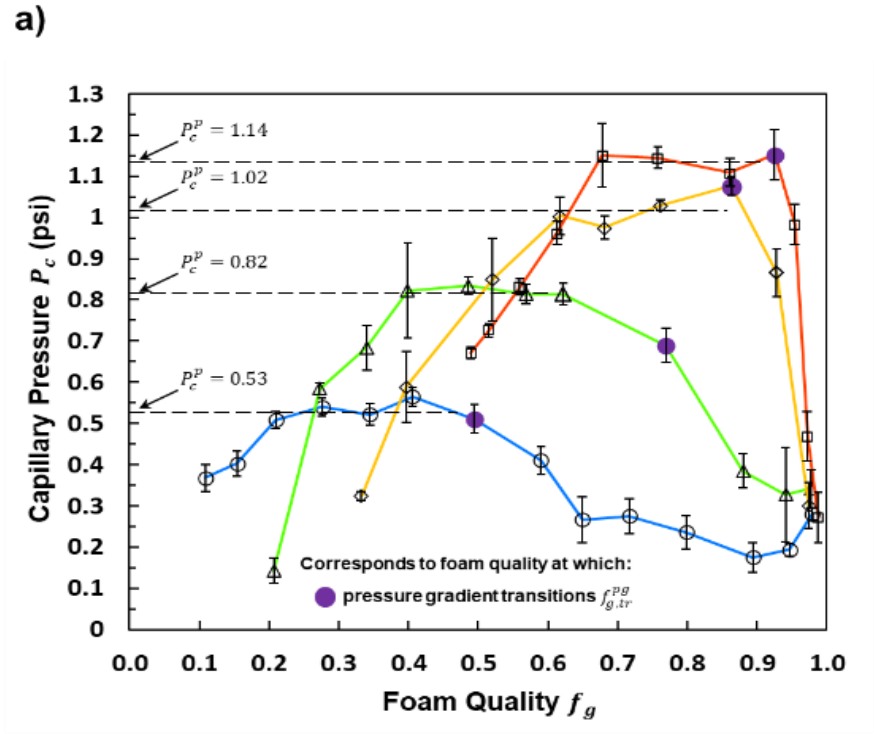

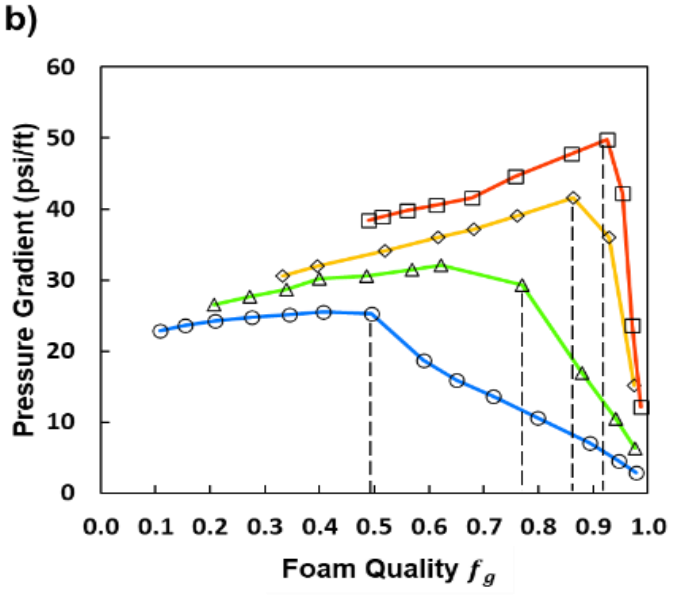

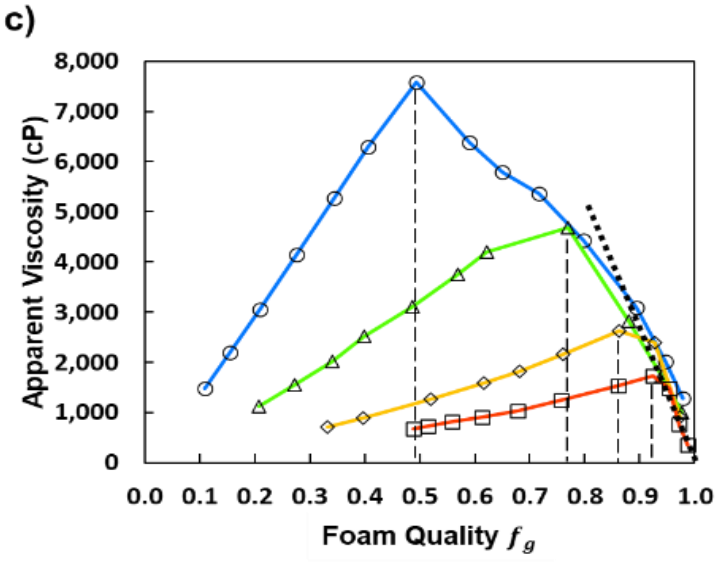

Vavra, et al., (2023), "Effects of velocity on N2 and CO2 foam flow with in-situ capillary pressure measurements in a high-permeability homogeneous sandpack", Scientific Reports

Foam generation in a consolidated core

557 md sandstone
AOS
f_g = 90%
u_T = 2.1 m/day

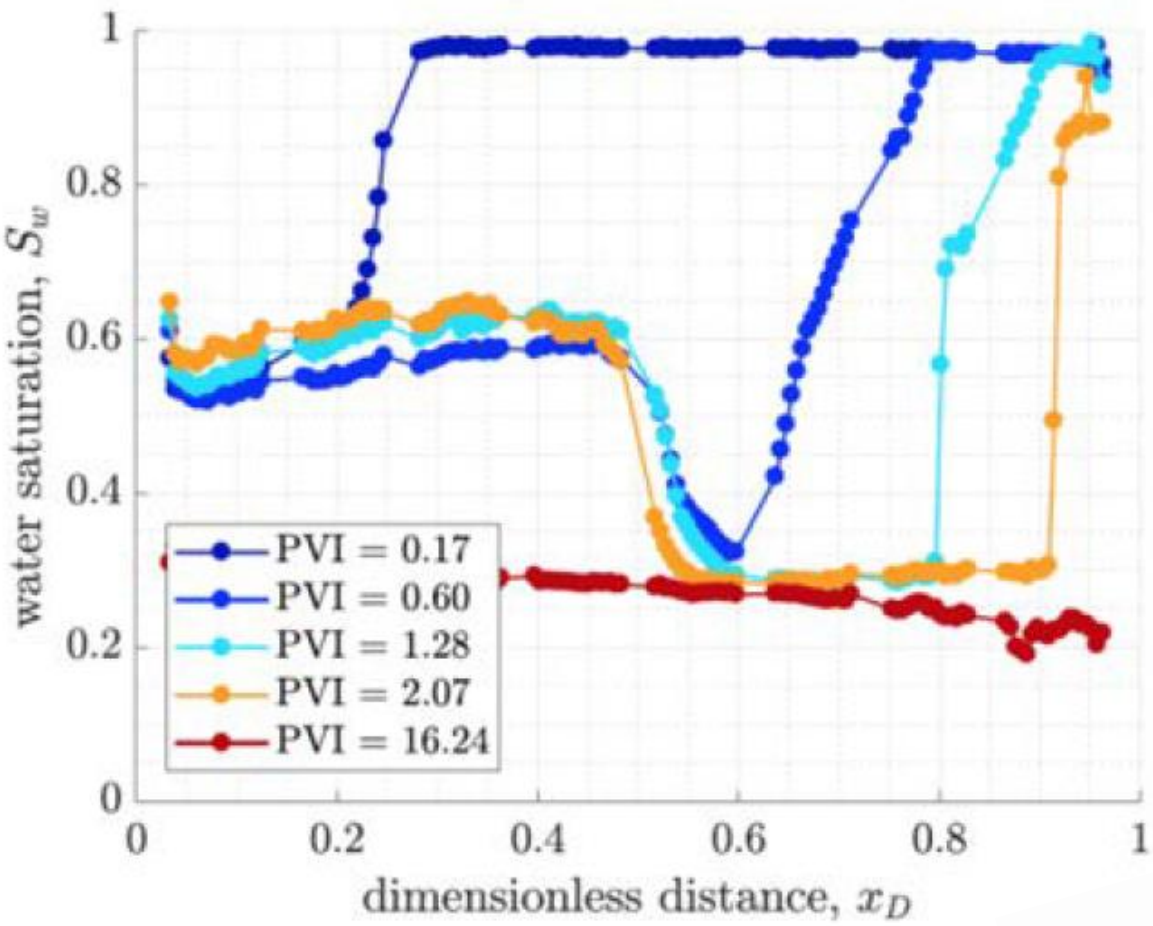

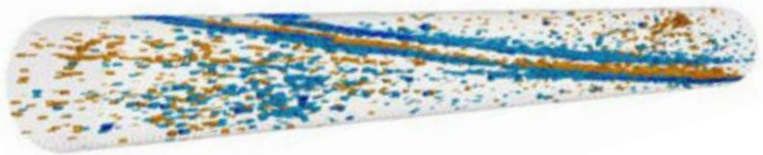

Almajid and Kovscek, 2022

Empirical foam model for reservoir simulation

- **CMG STARS foam model**
- **Gas mobility function of:**
  - **Water saturation (S_w)**
  - **Velocity (Capillary Number)**
  - **Surfactant concentration**
  - **Oil saturation**

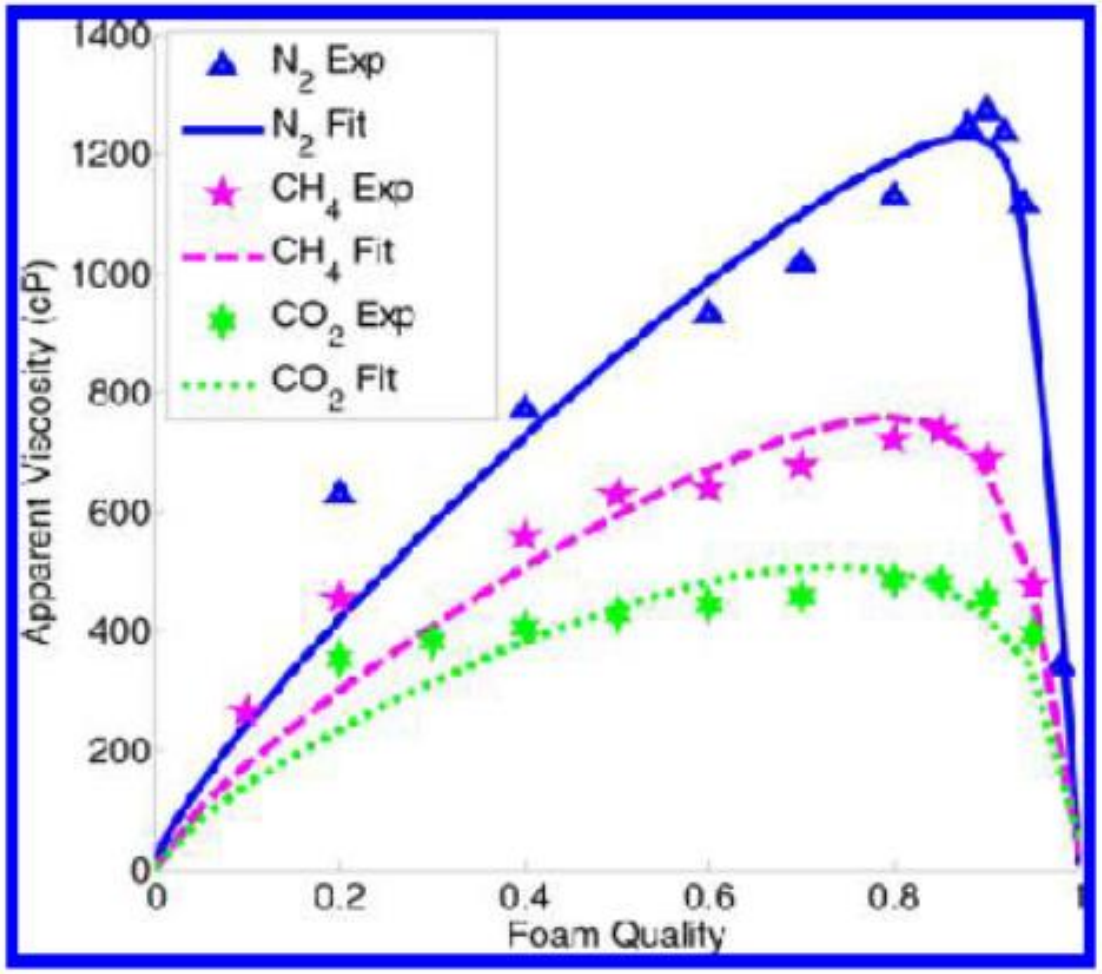

Figure 9. Data fit to STARS model for different gas type experiments.

Cheng, et al., 2000, SPE 59287
Zeng, et al., 2016, *Ind. Eng. Chem. Res., 55*

Experiments for field application

Evaluation at: 120 °C, 3,400 psi CO_2, 22% TDS, limestone
TTM is a C16 – C18 diamine, cationic surfactant

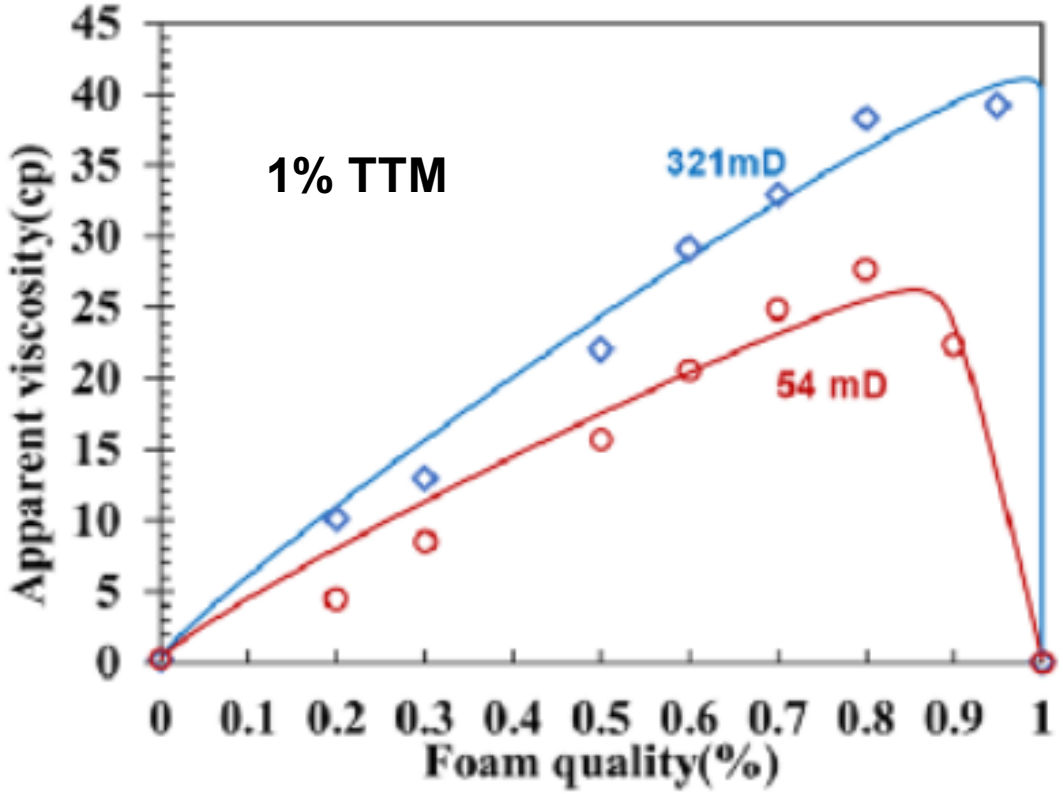

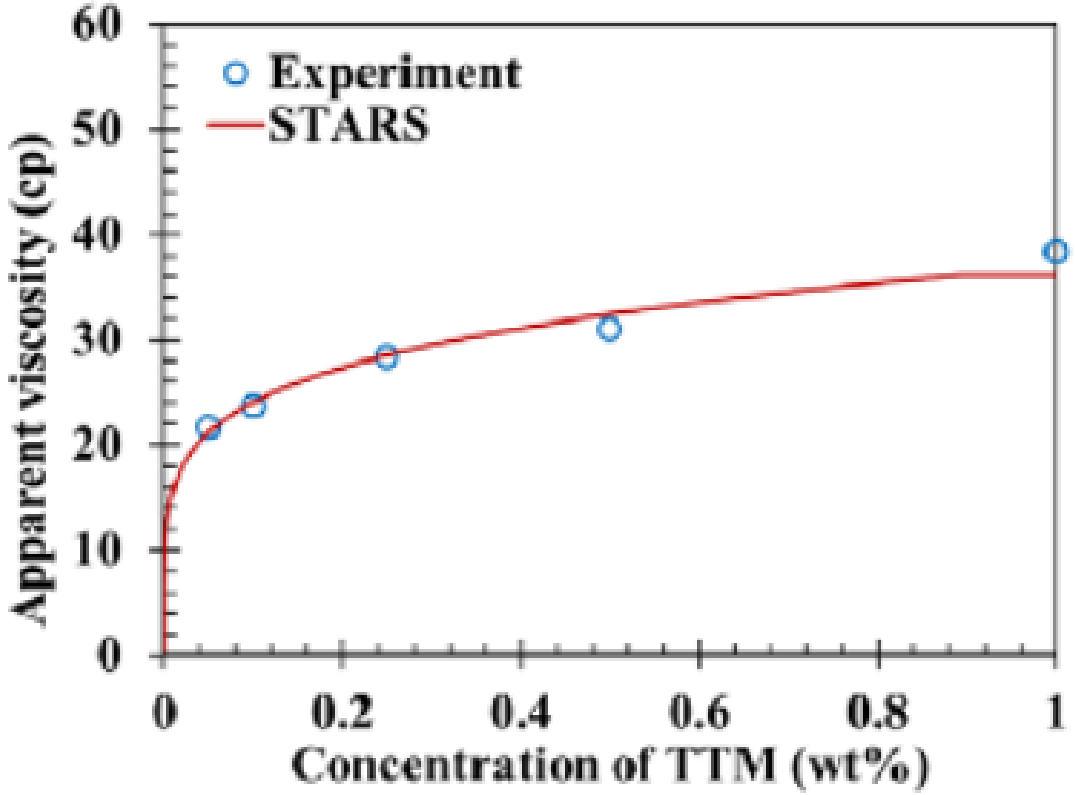

Jian, et al., 2020, *E&F*
Elhag, et al., 2014.

Simulations for field application

Cross-sectional view with horizontal wells
CO_2/TTM or CO_2/brine: upper left
CO_2 only lower left;

Producer; lower right

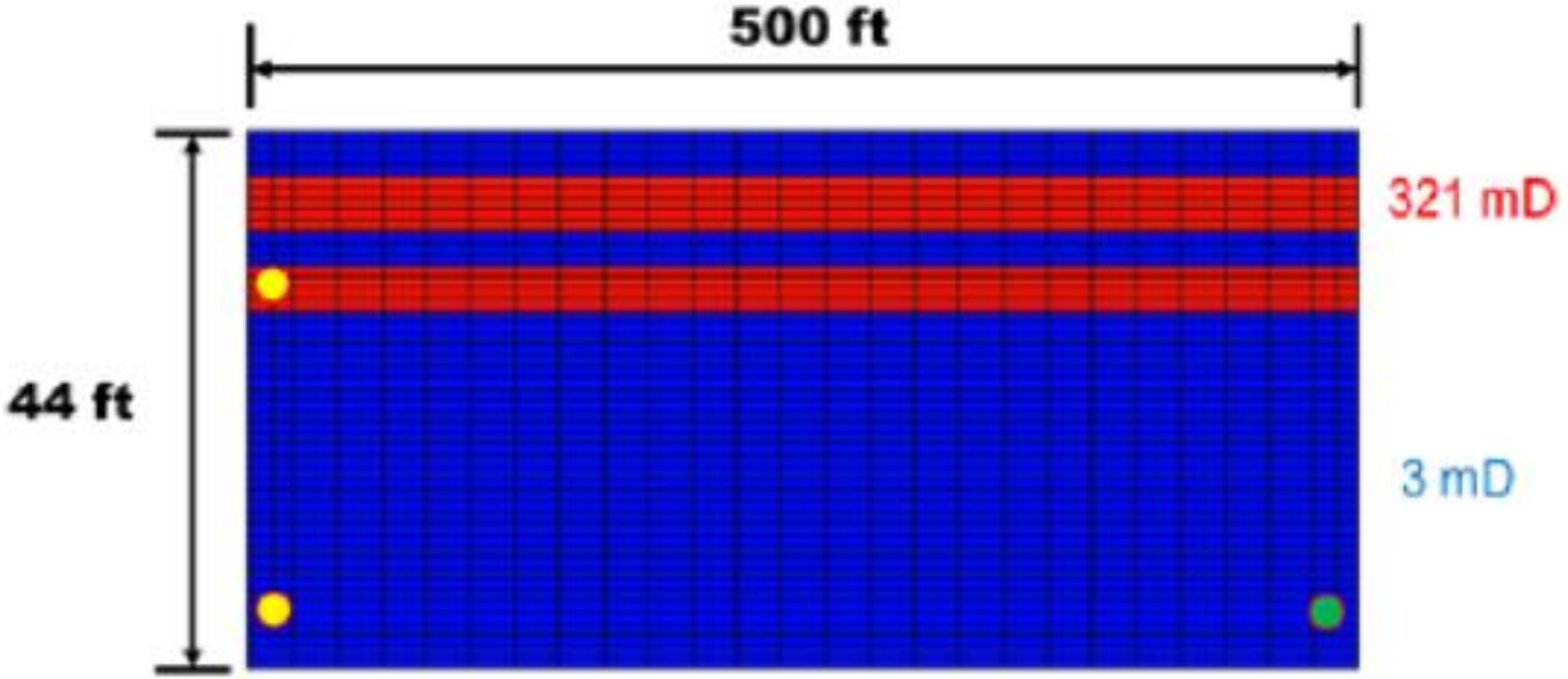

Jian, et al., 2020, *E&F*

Simulations for field application

CO_2 & brine injection
1, 2, 5,
8, 10, 15 years

(a)

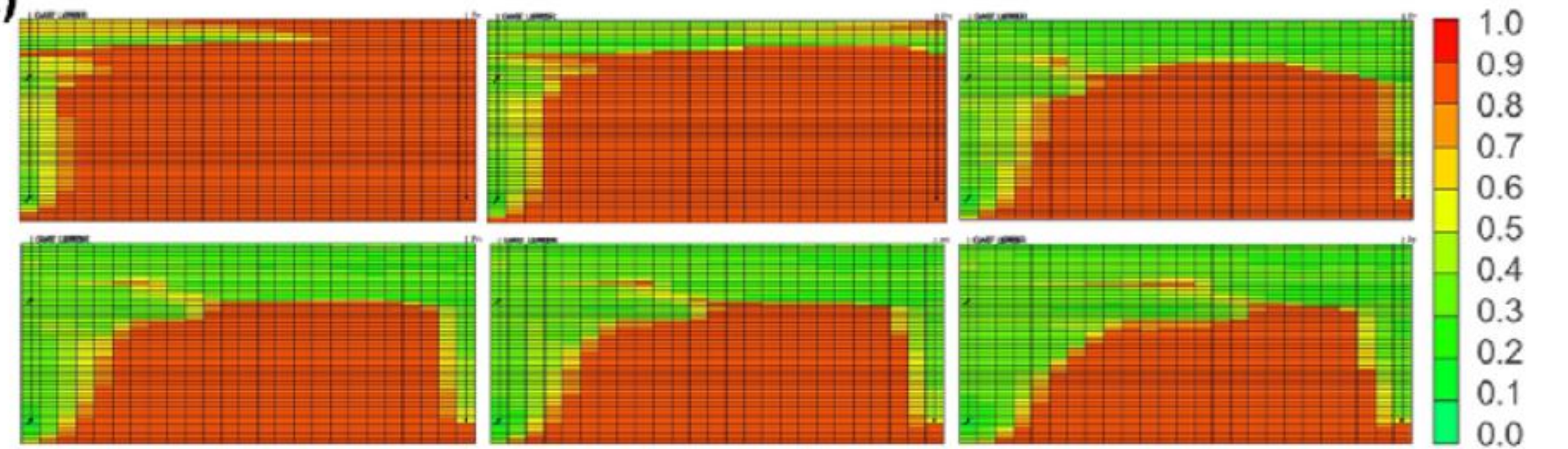

Jian, et al., 2020, *E&F*

Simulations for field application

CO_2 & 1% TTM foam injection
1, 2, 5,
8, 10, 15 years

Oil saturation

(b)

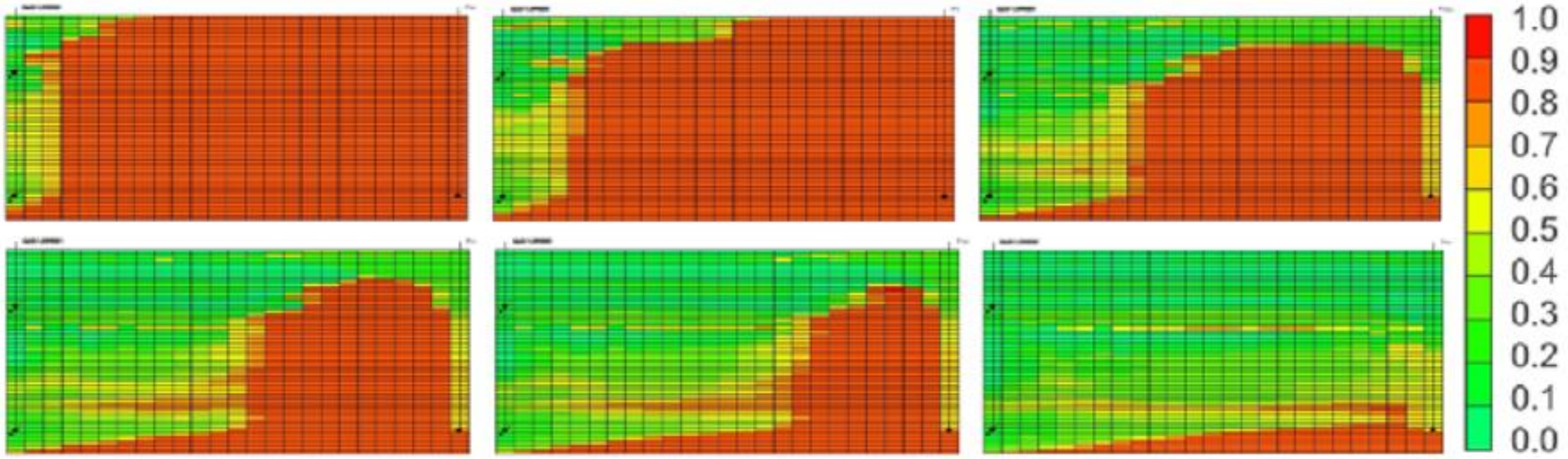

Jian, et al., 2020, *E&F*

Conclusions

- Choice of surfactant is essential
- Bubble size and distribution governs foam viscosity
- Bubble generation is governed by capillary heterogeneity and/or exceeding minimum pressure gradient
- Foam strength is limited by P_c and bubble generation
- Empirical models are available for fitting measurements and applying in simulators
- Reservoir simulators are available to evaluate benefit of foam mobility control for enhanced oil recovery

- Almajid, M. M., and Kovscek, A.R. (2022), “Experimental Investigation of Transient Foam Flow in a Long Heterogeneous Consolidated Sandstone,” SPE-209401-MS, SPE IOR virtual conference.
- Chen, et al. (2015), “CO_2-in-Water Foam at Elevated Temperature and Salinity Stabilized with a Nonionic Surfactant with a High Degree of Ethoxylation,” *I&EC Research, 54, 16*, 4252-4263.
- Cheng, L, et al., (2000), “Simulating Foam Processes at High and Low Qualities,” SPE 59287, paper presented at 2000 SPE/DOE IOR Symp., 3-5 April.
- Elhag, et al., (2014), “Switchable diamine surfactants for CO_2 mobility control in enhanced oil recovery and sequestration,” *Energy Procedia 63*, 7709-7716.
- Falls, A.H., et al., (1988), “Development of a Mechanistic Foam Simulator: The Population Balance and Generation by Snap-off,” *SPERE*, *Aug.*, 884-892.
- Falls, A.H., Musters, J.J., and Ratulowski, J., (1989), “The Apparent Viscosity of Foams in Homogeneous Bead Packs,” *SPERE*, *May*, 155-164.
- Farajzadeh, R., et al., (2015), “Effect of Permeability on Implicit-Texture Foam Model Parameters and the Limiting Capillary Pressure,” *Energy & Fuels, 29*, 3011-3018.
- Hirasaki, G.J., (1982). “Ion Exchange with Clays in the Presence of Surfactant,” SPEJ, April, 181-192.
- Hirasaki, G.J., and Lawson, J.D., (1985), “Mechanisms of Foam Flow in Porous Media: Apparent Viscosity in Smooth Capillaries,” *SPEJ*, *April*,176-190.
- Jian, G., et al., (2020), “Evaluating the Transport Behavior of CO_2 Foam in the Presence of Crude Oil under High-Temperature and High-Salinity Conditions for Carbonate Reservoirs,” *Energy & Fuels, 33*, 6038-6047.
- Rossen, W.R., Farajzadeh, R., and Hirasaki, G.J., (2024), " Potential and Challenges of Foam-Assisted CO2 Sequestration," *Geoenergy Science and Engineering, 239*, 212929.
- Svorstoel, I., et al., (1996), “Foam Pilot Evaluations for the Snorre Field,” 8th European *IOR Symposium,* Vienna, Austria*..*
- Svorstol, I., et al., (1996), “Laboratory Studies for Design of a Foam Pilot in the Snorre Field*,” SPE/DOE 35400*, Tulsa, OK.
- Tanzil, D., et al, (2002), “Mobility of Foam in Heterogeneous Media: Flow Parallel and Perpendicular to Stratifications,” *SPEJ, June*, 203-212.
- Vavra, E., et al., (2022), “Measuring in-situ capillary pressure of a flowing foam system in porous media,” *JCIS, 621*, 321-330.
- Vavra, E., et al., (2023), “Effects of velocity on N2 and CO2 foam flow with in-situ capillary pressure measurements in a high-permeability homogeneous sandpack,” Scientific Reports, 13:10029 .
- Yu, G., Vincent-Bonnieu, S., Rossen, W.R., (2020), “Foam Propagation at Low Superficial Velocity: Implications for Long-Distance Foam Propagation,” *SPEJ, Dec.*, 3457-3471.
- Zeng, Y., et al., (2016), “Insights on Foam Transport from a Texture-Implicit Local-Equilibrium Model with an Improved Parameter Estimation Algorithm,” *Ind. Eng. Chem. Res., 55*, 7819-7829.